Free-induction decay after a pulse saturation for systems with random telegraph frequency

V. S. Malinovsky
Institute of Thermophysics, Russian Academy of Sciences, Novosibirsk, 630090, Russia
(Received 21 February 1995; revised manuscript received 5 June 1995)

The free-induction decay (FID) after saturation by a laser radiation pulse of finite duration is studied for systems with spectral diffusion. The exact solution of the FID signal shape has been obtained in the framework of the telegraph noise model. This solution takes into account the finite duration of the saturating field and is valid at arbitrary values of the spectral exchange rate and the amplitude of the coherent field. The exact expression of the FID signal is derived in the weak-external-field limit. It is shown that the FID signal suddenly disappears after a time equal to the pulse width. This confirms the validity of the theorem on coherent transients, which has been proved for the Bloch equations [A. Schenzle, N. C. Wong, and R. G. Brewer, Phys. Rev. A **22**, 635 (1980)].

PACS number(s): 42.50.Md

I. INTRODUCTION

Recently, a number of experimental studies been published dealing with the investigation of phenomena that constitute the base of coherent nonlinear spectroscopy and saturation spectroscopy of solids, i.e., nutations [1], free-induction decay (FID) [2–4], rotary echo [5], hole burning [6,7], etc. All the studies have demonstrated the inapplicability of Bloch equations to the analysis of the effects mentioned above. This results from the fact that the Bloch equations incorrectly take into account the random modulation of impurity ion frequencies in solids. The frequency modulation of the transition excited by a laser radiation field is accounted for by the random reorientation of spins of the crystal lattice. The reorientation leads to a change in local fields and correspondingly, in impurity ion frequencies. The random frequency modulation connected with the dephasing perturbations evokes a relaxation in a system. The coherent field influences the dephasing processes. As a result, the relaxation coefficients depend on the amplitude and frequency of the field in the master equation for the density matrix averaged over the random perturbations. There is no such dependence in the Bloch scheme.

In this paper we restrict our theoretical discussions to the FID after saturation in random frequency modulation systems. To explain the experimental results obtained for the FID [2], a considerable number of theoretical studies have been offered in which the frequency modulation is simulated using the Markovian random processes. The studies [8–14] suggested different versions of the FID theory based on the idea of a fast spectral exchange. Such a theory is often referred to as a Gaussian-Markovian theory. A diffusion model for a frequency exchange (the Markovian correlated modulation) based on the numerical solution of the Fokker-Planck equation was described in [15]. A model of noncorrelated frequency modulation was presented in [16,17], followed by several exact solutions for a FID signal shape within the limits of suggested model [18]. The telegraph noise model (the Markovian anticorrelated modulation) was used to describe the FID in [19]. Later, in [20], an exact solution for a FID signal in the framework of the telegraph noise model was obtained and applicability limitations for the theory developed in [19] were found. It is to be indicated that for a FID signal the results obtained in a simplified telegraph noise model coincide with the results of the Gaussian-Markovian theory [8–14], this being a reason for the cases of their identification. A similar coincidence of results for these two models for the absorption as well as emission line shapes were mentioned in [21], where the fast spectral exchange theory (Gaussian-Markovian theory) was named the Born approximation.

A difference between the experimental studies [2] and [3] consists in the exciting radiation impulse duration ($T = 200$ μsec) being considerably shorter than the population relaxation time ($T = 4200$ μsec). All the theories mentioned above were developed for the FID signal after steady-state saturation, i.e., they cannot be employed to describe the results of [3].

To analyze the experimental data [3], a fast spectral exchange theory was used that took into account the saturating impulse duration. However, it did not allow an adequate description of the experimental dependence of the FID rate on the saturating radiation field strength to be made. To describe various transient coherent phenomena, in particular, the FID after pulse saturation, the telegraph noise model was suggested in [22]. The authors of that study [22] did not succeed in obtaining an exact solution for a FID signal shape and the analyses of experimental data were made on the basis of approximate calculations, resulting in a conclusion about slow spectral exchange in the system investigated. The purpose of this study is to present a general theory of a FID signal shape after saturation by a strong field impulse of arbitrary duration as well as to analyze experimental data [3] in the framework of an anticorrelated frequency modulation.

II. FID AFTER A PULSE SATURATION

Let us consider the ensemble of impurity ions that drives by a monochromatic radiation field $\mathscr{E}=E_0\exp\{i\omega t\}$ within the time T and interacts with a perturber reservoir. After immediately switching off the field a FID signal is observed. The polarization is induced during the radiation impulse.

 © 1995 The American Physical Society

Each impurity ion is to be modeled by a two-level system (TLS) whose frequency

$$E_2(t)-E_1(t)=\omega_0+\varepsilon(t)$$

is a stationary random process: its mean value ω_0 and equilibrium distribution $\varphi(\varepsilon)$ are conserved with respect to time [$E_{1,2}(t)$ are the energy levels of the TLS].

Since the value of ω_0 is distributed along the inhomogeneous contour $\Phi(\omega_0)$, caused by the crystal field dispersion, the FID signal shape is defined as

$$R(T+t)=\Phi_0 \mathrm{Im}\int d\Delta\omega\ \overline{\sigma_{12}(T+t,\Delta\omega)}\ , \tag{1}$$

where $\Delta\omega=\omega_0-\omega$ is the detuning frequency, ω is the saturating field frequency, $\Phi_0=\Phi(\omega_0=\omega)=$ const, and $\overline{\sigma_{12}(T+t,\Delta\omega)}$ is the off-diagonal element of a density matrix, which determines the polarization at the time moment t after switching off the field. The general expression for $\overline{\sigma_{12}(T+t,\Delta\omega)}$ has the form

$$\overline{\sigma_{12}(T+t,\Delta\omega)}=\left\langle \sigma_{12}(T,\Delta\omega)\exp\left\{ i\Delta\omega t+i\int_T^{T+t}\varepsilon(t')dt' -t/T_2\right\}\right\rangle\ , \tag{2}$$

where the angular brackets denote the averaging over random realizations of the process $\varepsilon(t)$, $\sigma_{12}(T,\Delta\omega)$ is the initial polarization induced by the saturating field, and T_2 takes into account the spontaneous decay of the excited level.

Usually when calculating $R(t)$, the correlation of the TLS frequency fluctuations before and after switching off the field is neglected. This makes possible the decoupling procedure in Eq. (2), averaging separately $\sigma_{12}(T,\Delta\omega)$ and exponent. As result, we obtain

$$\overline{\sigma_{12}(T+t,\Delta\omega)}=\overline{\sigma_{12}(T,\Delta\omega)}K(t)\ \exp\{i\Delta\omega t-t/T_2\}\ , \tag{3}$$

where

$$K(t)=\left\langle \exp\left\{ i\int_0^t\varepsilon(t')dt'\right\}\right\rangle \tag{4}$$

is the correlation function of a frequency modulation. In [18,20] it was indicated that if for the average $\overline{\sigma_{12}(T,\Delta\omega)}$ and $K(t)$ exact expressions are used, then for the FID signal shape results are obtained that are valid beyond the applicability range of the perturbations theory (PT) in the random detuning of a frequency. The condition for the PT to be applied, which corresponds to the fast frequency modulation limit, is

$$q^2=\overline{\varepsilon^2}\tau_0^2\ll 1\ , \tag{5}$$

where $\overline{\varepsilon^2}$ is the dispersion of the frequency distribution and τ_0^{-1} is the spectral exchange rate. It is in this framework of the approximation that the majority of theoretical efforts [8–14] to explain the experiments [3] were undertaken. It will be useful to note that the applicability range of Eq. (3) must be examined in every concrete case.

The expressions (1) and (2) are exact and determine the FID signal shape in a general case. It is not yet possible to carry out the averaging procedure defined in Eq. (2) in a generalized form. Therefore we concretize the random process $\varepsilon(t)$ and will later consider the case when the TLS frequency is modulated by the Markovian anticorrelated random process. This concretization of the random process $\varepsilon(t)$ allows the averaging in Eq. (2) to be performed and an exact expression for the FID signal shape to be obtained.

III. ANTICORRELATED MARKOVIAN FREQUENCY MODULATION

If the frequency of the TLS interacting with a laser radiation field is modulated by a purely discontinuous Markovian process, then, in agreement with the sudden modulation theory [23], the averaging in Eq. (2) can be represented as

$$\overline{\sigma_{12}(T+t,\Delta\omega)}=\exp\{i\Delta\omega t-t/T_2\}\int d\varepsilon K(\varepsilon,t)\sigma_{12}(\varepsilon,T)\ , \tag{6}$$

where $K(\varepsilon,t)$ and $\sigma_{12}(\varepsilon,T)$ are marginal or conditional averages, whose argument at switching off the field coincides and is equal to ε.

The subsequent consideration can be well performed in the Laplace presentation. Applying the Laplace transformation to Eq. (6), we get

$$\overline{\sigma_{12}(p,p_1,\Delta\omega)}=\int d\varepsilon K(\varepsilon,p_1)\sigma_{12}(\varepsilon,p), \tag{7}$$

where

$$K(\varepsilon,p_1)=\int_0^\infty dt\ K(\varepsilon,t)\exp\{-p_1t+i\Delta\omega t-t/T_2\}. \tag{8}$$

The frequency modulation function under anticorrelated spectral exchange was thoroughly investigated in [23]. Thus, for $K(\varepsilon,p_1)$ we immediately obtain the resulting expression

$$K(\varepsilon,p_1)=\frac{p_0+1/\tau_c+i\varepsilon}{p_0^2+p_0/\tau_c+\varepsilon^2}\ , \tag{9}$$

where $p_0=p_1+1/T_2-i\Delta\omega$, and τ_c is the correlation time, which is connected to τ_0 by the expression $\tau_0=2\tau_c$ for the anticorrelated exchange [14].

To obtain a general solution for a FID signal, we have to find $\sigma_{12}(\varepsilon,p)$ determining the polarization induced by a radiation field as function ε. For this purpose we will use kinetic equations of the Markovian sudden modulation theory [23]. Considering that under anticorrelated modulation the random variable ε may have only two values a and $-a$ and the probability density of the appearance of frequency ε after ε' is $f(\varepsilon',\varepsilon)=\delta_{\varepsilon',\varepsilon}$, the equation for the density matrix should be presented in the form

$$\dot{X}(a)=-\left[\hat{L}_0+\frac{1}{2\tau_c}+ia\hat{L}_1\right]X(a)+\frac{1}{2\tau_c}X(-a)+\hat{\Lambda}\varphi(a),$$

$$\dot{X}(-a)=-\left[\hat{L}_0+\frac{1}{2\tau_c}-ia\hat{L}_1\right]X(-a)+\frac{1}{2\tau_c}X(a)+\hat{\Lambda}\varphi(-a), \tag{10}$$

where

$$X=\begin{pmatrix}\sigma_{12}\\ \sigma_{21}\\ n\end{pmatrix},\quad \hat{L}_0=\begin{pmatrix}\frac{1}{T_2}-i\Delta\omega & 0 & -\frac{i\chi}{2}\\ 0 & \frac{1}{T_2}+i\Delta\omega & \frac{i\chi}{2}\\ -i\chi & i\chi & \frac{1}{T_1}\end{pmatrix},$$

$$\hat{L}_1=\begin{pmatrix}-1&0&0\\0&1&0\\0&0&0\end{pmatrix},\quad \hat{\Lambda}=\begin{pmatrix}0\\0\\\frac{n_0}{T_1}\end{pmatrix},$$

$\sigma_{12}=\sigma_{21}^*=\rho_{12}\exp\{i\omega t\}$, $n=\rho_{22}-\rho_{11}$ is the population difference, n_0 is the equilibrium population difference, $\chi=d_{12}E_0$ is the Rabi frequency, T_1 and T_2 are the times of longitudinal and transversal relaxation accounted for by a spontaneous decay, and $\varphi(\varepsilon)=0.5\delta_{\varepsilon,a}+0.5\delta_{\varepsilon,-a}$ is a static equilibrium frequency distribution.

For further consideration it is reasonable to use the expressions

$$\bar{X}=[X(a)+X(-a)]/2,$$
$$X_A=[X(a)-X(-a)]/2. \tag{11}$$

Then Eq. (10) can be transformed into

$$\dot{\bar{X}}=-\hat{L}_0\bar{X}-ia\hat{L}_1X_A+\hat{\Lambda},$$
$$\dot{X}_A=-[\hat{L}_0+1\tau_c]X_A-ia\hat{L}_1\bar{X}. \tag{12}$$

Applying to these equations the Laplace transformation, we obtain

$$\bar{X}(p)=\left[p+\hat{L}_0+a^2\hat{L}_1\frac{1}{p+\hat{L}_0+\frac{1}{\tau_c}}\hat{L}_1\right]^{-1}\left[X(0)+\frac{\hat{\Lambda}}{p}\right],$$

$$X_A(p)=-ia\left[p+\hat{L}_0+\frac{1}{\tau_c}\right]^{-1}\hat{L}_1\bar{X}(p). \tag{13}$$

Using Eqs. (13) and (11), we find the expression for the marginal density matrix element

$$X(\varepsilon,p)=\left(1-i\varepsilon\frac{1}{p+\hat{L}_0+\frac{1}{\tau_c}}\hat{L}_1\right)\times\left[p+\hat{L}_0+a^2\hat{L}_1\frac{1}{p+\hat{L}_0+\frac{1}{\tau_c}}\hat{L}_1\right]^{-1}\times 2\varphi(\varepsilon)\left[X(0)+\frac{\hat{\Lambda}}{p}\right]. \tag{14}$$

Employing the expressions for $\hat{L}_0$, $\hat{L}_1$, $\hat{\Lambda}$ in Eq. (14), we obtain

$$\sigma(\varepsilon,p)=\frac{n_0\chi\varphi(\varepsilon)}{p}\left\{-\Delta\omega^3+i\Delta\omega^2\left(p+\frac{1}{T_2}\right)+\Delta\omega(\varepsilon^2-\kappa^2)+i\kappa^2\left(p+\frac{1}{T_2}\right)+i\varepsilon^2(p+t_2)+\varepsilon\left[\Delta\omega^2-i\Delta\omega\left(2p+t_2+\frac{1}{T_2}\right)-\kappa^2\frac{p+\frac{1}{T_2}}{p+t_2}-\varepsilon^2\right]\right\}[\Delta\omega^4+B\Delta\omega^2+C]^{-1}, \tag{15}$$

where

$$B=\kappa^2-2a^2+\left(p+\frac{1}{T_2}\right)^2+\chi^2\frac{p+\frac{1}{T_2}}{p+\frac{1}{T_1}},$$

$$C=\left[\kappa\left(p+\frac{1}{T_2}\right)+a^2\frac{p+t_2}{\kappa}\right]\left[\kappa\left(p+\frac{1}{T_2}\right)+a^2\frac{\kappa}{p+t_2}+\chi^2\frac{\kappa}{p+\frac{1}{T_1}}\right],$$

$$\kappa^2=(p+t_2)^2+\chi^2\frac{p+t_2}{p+t_1},\quad t_{1,2}=\frac{1}{\tau_c}+\frac{1}{T_{1,2}}.$$

Performing the integration by ε defined by Eq. (7) and considering Eqs. (9) and (15), we have

$$\overline{\sigma_{12}(p,p_1,\Delta\omega)}=K(p_1)\overline{\sigma_{12}(p,\Delta\omega)}+K'(p_1)\sigma_{12}^{A}(p,\Delta\omega), \tag{16}$$

where

$$K(p_1)=\int d\varepsilon K(\varepsilon,p_1)\varphi(\varepsilon)=\frac{p+\dfrac{1}{\tau_c}}{p_1^2+\dfrac{p_1}{\tau_c}+a^2},$$

$$K'(p_1)=-\frac{a^2}{p_1^2+\dfrac{p_1}{\tau_c}+a^2},$$

$$\overline{\sigma_{12}(p,\Delta\omega)}=\frac{n_0\chi}{2p}\,\frac{-\Delta\omega^3+i(\Delta\omega^2+\kappa^2)\left(p+\dfrac{1}{T_2}\right)-\Delta\omega(\kappa^2-a^2)+ia^2(p+t_2)}{\Delta\omega^4+B\Delta\omega^2+C},$$

$$\sigma_{12}^{A}(p,\Delta\omega)=\frac{n_0\chi}{2p}\,\frac{-\Delta\omega^2+\Delta\omega\left(2p+t_2+\dfrac{1}{T_2}\right)+i\kappa^2\dfrac{p+\dfrac{1}{T_2}}{p+t_2}+ia^2}{\Delta\omega^4+B\Delta\omega^2+C}.$$

After performing an inverse Laplace transformation by p_1 and integrating by $\Delta\omega$ in accordance with the general expression (1), the FID signal shape can be described by

$$\begin{aligned}R(p,t)=\frac{\pi\Phi_0 n_0\chi}{2pD}\exp\left\{-\frac{t}{T_2}\right\}\{&K(t)[R_1(p)K_1(p,t)\\&+R_2(p)\dot{K}_1(p,t)]\\&+\dot{K}(t)[R_3(p)K_1(p,t)+R_4(p)\dot{K}_1(p,t)]\},\end{aligned} \tag{17}$$

where

$$K(t)=[p_1\exp\{p_2t\}-p_2\exp\{p_1t\}]/(p_1-p_2),$$

$$K_1(p,t)=[\Delta\omega_1\exp\{i\Delta\omega_2t\}-\Delta\omega_2\exp\{i\Delta\omega_1t\}]/(\Delta\omega_1-\Delta\omega_2),$$

$$p_{1,2}=-\frac{1\pm\lambda}{2\tau_c},\quad \lambda=\sqrt{1-4a^2\tau_c^2},$$

$$\Delta\omega_{1,2}=\begin{cases}\dfrac{i}{\sqrt{2}}\sqrt{B\pm\sqrt{B^2-4C}}, & B^2\geq 4C\\ \frac{1}{2}[\pm\sqrt{2\sqrt{C}-B}+i\sqrt{2\sqrt{C}+B}], & B^2<4C,\end{cases}$$

$$R_1=\kappa^2(p+1/T_2)+a^2(p+t_2)+\sqrt{C}[p+1/T_2-\sqrt{2\sqrt{C}+B}],$$

$$R_2=\kappa^2-a^2-\sqrt{C}-B+(p+1/T_2)\sqrt{2\sqrt{C}+B},$$

$$R_3=a^2+\kappa^2\frac{p+1/T_2}{p+t_2}-\sqrt{C},$$

$$R_4=2p+t_2+1/T_2-\sqrt{2\sqrt{C}+B},\quad D=\sqrt{C}\sqrt{2\sqrt{C}+B}\ .$$

Equation (17) is exact and determines the FID signal shape after saturation by a strong-field impulse under anticorrelated frequency modulation. The expression obtained is valid for the arbitrary strength of the saturating field and the arbitrary transition frequency modulation rate. We mention that having performed the boundary transition

$$R^s(t)=\lim_{p\to 0}pR(p,t), \tag{18}$$

we obtain the expression for the FID signal shape in the case of steady-state saturation [20]. Naturally, there is the possibility of comparing this result to the one we obtained within the range of $T\gg T_1$ and thus tracing the reaching of a steady-state saturation.

If in the framework of this model the TLS frequency modulation correlation before and after switching off the field be neglected, as performed in [19] then, in accordance with Eqs. (3) and (4), we get

$$\begin{aligned}R(p,t)=\frac{\pi\Phi_0 n_0\chi}{2pD}\exp\left\{-\frac{t}{T_2}\right\}&K(t)[R_1(p)K_1(p,t)\\&+R_2(p)\dot{K}_1(p,t)].\end{aligned} \tag{19}$$

It is evident from comparing Eqs. (19) and (17) that the appearance of the second term proportional to $\dot{K}(t)$ in the exact solution (17) is connected with taking into account the correlation of the TLS frequency fluctuations before and after switching off the field.

It should be emphasized that the expressions for the density-matrix elements, averaged by the random process realizations in the telegraph noise model [19,20], are identical

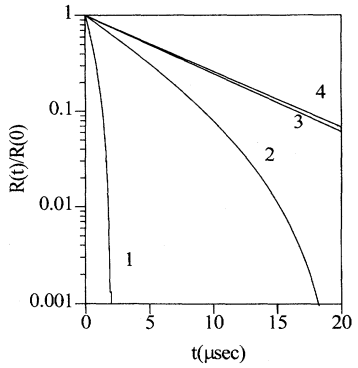

FIG. 1. FID signals vs time obtained from the Bloch equation as $\chi \to 0$. Longitudinal and transversal relaxation times are equal to 4200 μ sec and 15 μ sec, respectively. The duration of the excitation pulse is 1, $T=2\mu$sec; 2, $T=20$ μsec; 3, $T=200$ μ sec; 4, steady-state regime.

to the results of the non-Markovian perturbations theory in the random frequency detuning $\varepsilon(t)$ [11,14]. As a result, the expression for the FID signal shape within the range of a fast spectral exchange [Eq. (5)] coincides with the expression (19), where it is necessary to set $K(t)=\exp\{-\overline{\varepsilon^2}\tau_c t\}$ [23].

IV. SHAPE OF THE FID SIGNAL AFTER SATURATION

The final expressions for the FID signal shape contain two independent parameters a and τ_c. To determine these values by a theoretical explanation of experiments on the field dependence of the FID rate, experimental data on the photon echo are usually employed. In the anticorrelated frequency modulation model the echo signal shape is determined by the expression [24]:

$$V(t)=\exp\left\{-\left(\frac{1}{T_2}+\frac{1}{2\tau_c}\right)t\right\}\left[\frac{1-\lambda}{2}\exp\left\{-\frac{t\lambda}{2\tau_c}\right\}+\frac{1+\lambda}{2}\exp\left\{\frac{t\lambda}{2\tau_c}\right\}-4a^2\tau_c^2\right]\Big/\lambda^2. \tag{20}$$

It is seen, that the echo signal is exponential in the case of a fast spectral exchange [Eq. (5)] as well as in the case of a slow exchange ($a^2\tau_c^2 \gg 1$). In these cases the echo signal rate is equal to

$$\gamma_e=\begin{cases} 1/T_2+a^2\tau_c, & a^2\tau_c^2 \ll 1 \\ 1/T_2+1/2\tau_c, & a^2\tau_c^2 \gg 1. \end{cases} \tag{21}$$

Thus, if a echo signal is exponential we can determine either $a^2\tau_c$, presupposing a fast spectral exchange, or $1/2\tau_c$, presupposing a slow spectral exchange.

It should be noted that the field dependence of the FID rate as $\chi \to 0$ is added by the experimental data on the decay rate of the photon echo in studies dealing with the investigation of the FID. In [25] the expressions for the FID signal

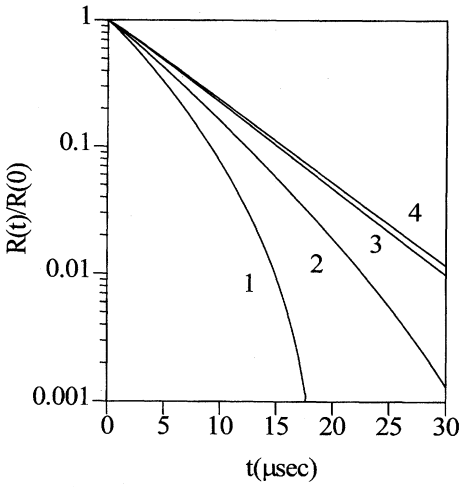

FIG. 2. FID signals vs time under fast frequency modulation as $\chi \to 0$. $a^2\tau_c^2=0.1$, $T_1=4200$ μsec, and $\gamma_e^{-1}=15$ μsec. The duration of the excitation pulse is 1, $T=20$ μsec; 2, $T=40$ μsec; 3, $T=200$ μsec; 4, steady-state regime.

after steady-state excitation as $\chi \to 0$ is obtained in the framework of different spectral exchange models under conditions indicated by Eq. (21). In this connection the analysis of the FID signal shape as $\chi \to 0$ under arbitrary value of spectral exchange rate will be of interest. Before the analysis of the FID signal in the telegraph noise model we examine the results obtained from the Bloch equations.

The Bloch equations can be presented as

$$\dot{X}=-\hat{L}_0 X+\hat{\Lambda}, \tag{22}$$

where

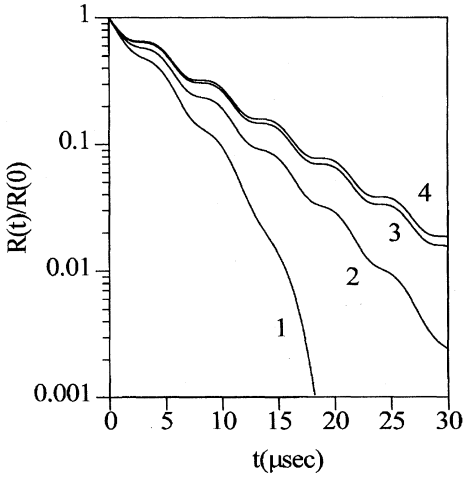

FIG. 3. FID signals vs time under slow frequency modulation as $\chi \to 0$. $a^2\tau_c^2=20$, $T_1=4200$ μsec, and $\gamma_e^{-1}=15$ μsec. The duration of the excitation pulse is 1, $T=20$ μsec; 2, $T=40$ μsec; 3, $T=200$ μsec; 4, steady-state regime.

$$X=\begin{pmatrix}\sigma_{12}\\ \sigma_{21}\\ n\end{pmatrix},$$

$$\hat{L}_0=\begin{pmatrix}\frac{1}{T_2^*}-i\Delta\omega & 0 & -\frac{i\chi}{2}\\ 0 & \frac{1}{T_2^*}+i\Delta\omega & \frac{i\chi}{2}\\ -i\chi & i\chi & \frac{1}{T_1}\end{pmatrix},\quad \hat{\Lambda}=\begin{pmatrix}0\\ 0\\ n_0/T_1\end{pmatrix},$$

T_2^* is the time of the transversal relaxation, and T_1 is the lifetime of the excited state. Applying the Laplace transformation to these equations we have

$$X(p)=\frac{1}{p+\hat{L}_0}[X(0)+\hat{\Lambda}/p]. \tag{23}$$

Using Eq. (23), the expression for the off-diagonal element of the density matrix can easily be obtained

$$\sigma_{12}(p)=\frac{n_0}{2p}\,\frac{i\chi(p+1/T_2^*+i\Delta\omega)}{\Delta\omega^2+(p+1/T_2^*)^2+\chi^2(p+1/T_2^*)/(p+1/T_1)}.$$

Substituting this expression into Eqs. (1) and (2), we find the expression for the Laplace image of the FID signal

$$R(p,t)=\frac{n_0\chi\pi\Phi_0}{2p}\,\frac{p+1/T_2^*-G(p)}{G(p)}\,\exp\{-t/T_2^*-tG(p)\}, \tag{24}$$

where

$$G(p)=\{(p+1/T_2^*)^2+\chi^2(p+1/T_2^*)/(p+1/T_1)\}^{1/2}.$$

The expression (24) indicates that the well-known result for the FID signal after steady-state saturation can be derived [26] in limit (18). The third-order contribution in χ, obtained from the formula (24), is

$$R(p,t)=-\chi^3\frac{n_0\pi\Phi_0}{4p(p+1/T_1)(p+1/T_2^*)}\,\exp\{-2t/T_2^*-pt\}. \tag{25}$$

Finally, performing an inverse Laplace transformation by p, a simple expression can be found

$$R(T,t)=\begin{cases}-\chi^3\frac{n_0\pi\Phi_0T_1T_2^*}{4}\exp\{-2t/T_2^*\}\left(1-\frac{T_1}{T_1-T_2^*}\exp\left\{\frac{t-T}{T_1}\right\}+\frac{T_2^*}{T_1-T_2^*}\exp\left\{\frac{t-T}{T_2^*}\right\}\right), & T>t\geq 0\\ 0, & T<t.\end{cases} \tag{26}$$

From either Eq. (26) or Eq. (25), using the limit $T\to\infty$ or relation (18), for the FID signal shape after steady-state excitation (at $\chi\to 0$) we find

$$R^s(t)=-\chi^3\frac{n_0\pi\Phi_0T_1T_2^*}{4}\,\exp\{-2t/T_2^*\}. \tag{27}$$

Figure 1 shows shape signals of the FID [Eq. (26)] in the weak-external-field limit under different duration of coherent pulse. The FID signal after steady-state excitation and the FID signal after excitation by pulse of finite duration $T\approx T_1$ are exponential with the decay rate $2/T_2^*$. But the FID signal becomes nonexponential with decreasing pulse duration.

Using Eq. (17), for the FID signal under the frequency modulation by the Markovian anticorrelated process in the third-order contribution in χ we obtain

$$R(p,t)=-\chi^3\frac{n_0\pi\Phi_0}{4}\exp\{-(p+2/T_2)t\}F(p,t), \tag{28}$$

where

$$F(p,t)=\frac{1}{p(p+1/T_1)(p+t_1)D}\left\{[(p+t_2)(p+t_1)(2p+t_2+1/T_2)+a^2(2p+t_1+1/T_1)]K^2(t)\right.$$
$$\left.+\frac{2}{\tau_c}(2p+t_1+1/T_2)K(t)\dot{K}(t)+\left[2p+t_1+1/T_1+\frac{(2p+t_2+1/T_2)(p+1/T_2)(p+1/T_1)}{a^2}\right]\dot{K}^2(t)\right\},$$

$$D=(2p+t_2+1/T_2)[a^2+(p+t_2)(p+1/T_2)].$$

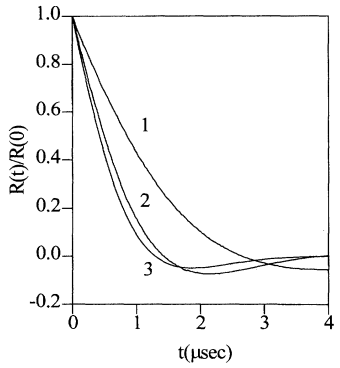

FIG. 4. FID signals vs time under fast frequency modulation. $a^2\tau_c^2=0.1, \chi/2\pi=50$ kHz, $T_1=4200$ μsec, and $\gamma_e^{-1}=15$ μsec. The duration of the saturation pulse is 1, $T=200$ μsec; 2, $T=2000$ μsec, 3, steady-state saturation.

So we can present the FID signal shape as

$$R(T,t)=\begin{cases} -\chi^3\dfrac{n_0\pi\Phi_0}{4}\ \exp\{-2t/T_2\}f(T-t), & T>t\geq 0 \\ 0, \quad T<t, \end{cases}$$

where

$$f(T-t)=\frac{1}{2\pi i}\int_{b-i\infty}^{b+\infty}\exp\{p(T-t)\}F(p,t)dp.$$

Taking into account the form $F(p,t)$, we can write the expression for the FID signal as $\chi\to 0$ under $T>t\geq 0$ as

$$R(T,t)=-\chi^3\frac{n_0\pi\Phi_0}{4}\ \exp\{-(2/T_2+1/\tau_c)t\}$$
$$\times\sum_{j=1}^{6}B_j(t)\exp\{p_j(T-t)\}, \qquad (29)$$

where p_j are the roots defined by the characteristic equations

$$p(p+1/T_1)(p+t_1)(2p+t_2+1/T_2)[a^2+(p+t_2)(p+1/T_2)]$$
$$=0.$$

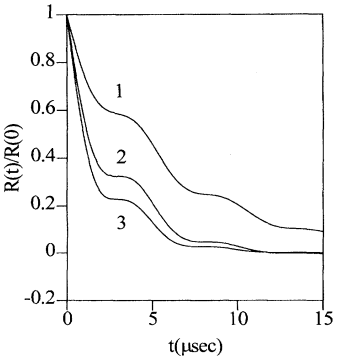

FIG. 5. FID signals vs time under slow frequency modulation. $a^2\tau_c^2=20$, $\chi/2\pi=5$ kHz, $T_1=4200$ μsec, and $\gamma_e^{-1}=15$ μsec. The duration of the saturation pulse is 1, $T=200$ μsec; 2, $T=2000$ μsec; 3, steady-state saturation.

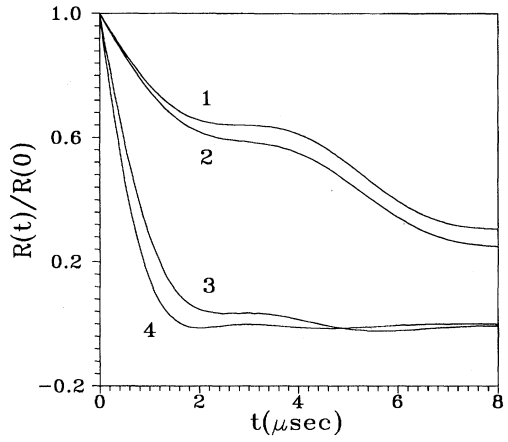

FIG. 6. FID signals vs time under slow frequency modulation. $a^2\tau_c^2=20$, $T_1=4200$ μsec, $\gamma_e^{-1}=15$ μsec, and $T=200$ μsec. The Rabi frequencies are 1, $\chi/2\pi=0.5$ kHz; 2, $\chi/2\pi=5$ kHz; 3, $\chi/2\pi=50$ kHz; 4, $\chi/2\pi=100$ kHz.

The expression of the FID signal is unwieldy, so we do not lead it. The FID signal shapes under different duration of excitation pulse in the framework of the telegraph noise model are shown in Figs. 2 and 3. Figure 2 presents the results for fast frequency modulation and Fig. 3 presents the results for slow modulation of TLS frequency. The behavior of the FID signal is the same with the results obtained on the basis of the Bloch equations. It is seen that the FID signal suddenly disappears after a time equal to the pulse duration. This type of behavior has been discussed theoretically [27–29] and has been observed experimentally [30]. Qualitatively, the effect is connected to the fact that a pulse of duration T excites a frequency band of $\sim\pi/T$. The dipoles then dephase completely in a time T, which is the Fourier transform of the bandwidth.

It should be emphasized that as $\chi\to 0$ the theorem on coherent transients [29] is valid for the Bloch representation [Eq. (26)] as well as for the telegraph noise model [Eq. (29)]. In addition, taking into account that the FID decay rate increases with increasing Rabi frequency, we can make the conclusion that this theorem is valid at arbitrary Rabi frequency.

To analyze the FID signal shape after saturation by a finite duration impulse, we employed an algorithm for the Laplace numerical inverse transformation, described in [31]. This algorithm has been tested when performing the inverse Laplace transformations and has yielded good results. In addition, the correctness of performing the numerical transformation of $R(p,t)$ will be tested by comparing the results in the case of $T\gg T_1$, when the exact analytical solution for the FID signal is known [20].

Figures 4 and 5 demonstrate the FID signal shape calculated for different saturation impulse durations. For comparison, a FID signal shape after a steady-state saturation is shown. It is indicated that when the saturating impulse duration increases, i.e., with $T\to T_1$, the FID signal shape approaches the after-steady-state saturation shape. This fact has been employed to test the accuracy of the calculations performed. It is to be noted that the result is true for the case of

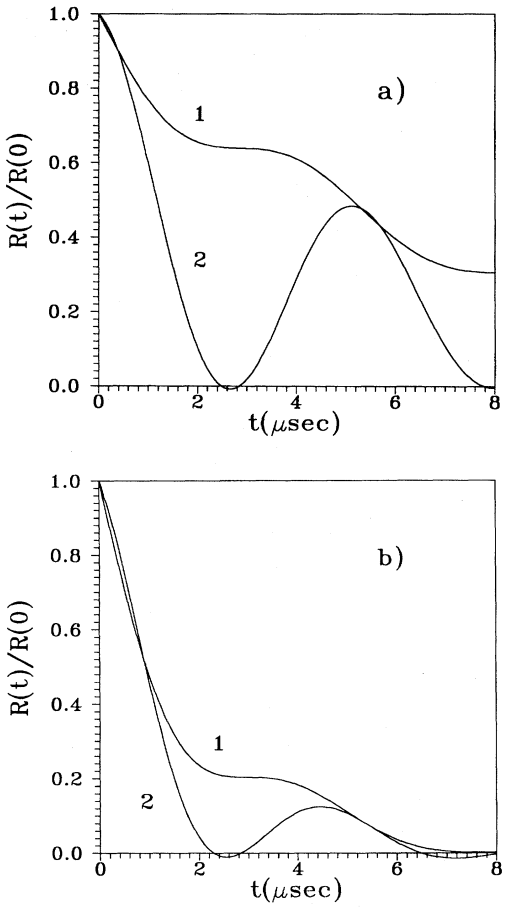

FIG. 7. FID signals vs time. $a^2\tau_c^2 = 20$, $T_1=4200$ μsec, $\gamma_e^{-1}= 15$ μsec, and $T=200$ μsec. The equations are 1, the exact solution [Eq. (17)]; 2, the approximate solution [Eq. (19)]. (a) $\chi/2\pi=0.5$ kHz and (b) $\chi/2\pi=20$ kHz.

a fast exchange (Fig. 4) and for the case of a slow exchange (Fig. 5). It should be emphasized that the condition $T \gg \gamma_e$ with $T_1 > T$ is far from being sufficient to employ the expressions for an after-steady-state saturation FID signal shape, as used in [4].

Figure 6 shows examples of the calculations obtained for various Rabi frequencies. It demonstrates the influence of a saturating field strength on the FID kinetics. As the Rabi frequency increases the decay rate of the induced polarization is accelerated and the modulation caused by the spectral exchange in the system is reduced. The increase of the FID rate with increasing Rabi frequency is connected to the power broadening of the hole width burned into the inhomogeneous profile during the preparation. The more intensive the field burns, the wider the hole, further, the FID rate increases after switching off the field. However, the spectral exchange leaves traces on the decay kinetics by means of a modulation. The modulation is strongly marked when spectral exchange is slow (Fig. 5 and 6). At the fast frequency exchange the shape of the burned hole has a nearly Lorentzian profile and correspondingly the FID kinetics becomes like the exponential kinetics in an initial stage (Fig. 4).

Figures 7(a) and 7(b) show the FID signal calculated according to the exact equation (18) as well as the approximate equation (20). It is seen that we have to take into consideration the correlation of the TLS frequency fluctuations before and after switching off the field. We should note that the difference between exact and approximate solutions is reduced by increasing the Rabi frequency. This reflects the power- broadened linewidth that was burned into the inhomogeneous profile during the preparation.

V. CONCLUSION

The exact solution of the FID signal shape after saturation by a radiation pulse of finite duration under anticorrelated spectral exchange is obtained. The analysis of the FID signal at an arbitrary rate of the spectral exchange and at an arbitrary Rabi frequency is fulfilled. It is shown that the correlation of the fluctuations before and after switching off the field must be taken into consideration.

The FID signal shape has been calculated by implying the conditions of [3]. It was performed to demonstrate the fact that the exact solution for the FID signal in a telegraph noise model produces a nonexponential decay, in contrast to the experimental data and approximate calculations performed in [22]. Thus an approximate solution providing an exponential decay of induced polarization cannot claim to explain the experiments [3]. In all probability, simplifications used in [22] have lead to qualitative changes of the calculated FID signal kinetics.

The exact analytic expression of the FID signal is derived in the weak-external-field limit. This expression is valid at an arbitrary rate of frequency modulation. It is shown that decreasing the saturation pulse duration leads to nonexponential decay of induced polarization actually at limits $a\tau_c \ll 1$ and $a\tau_c \gg 1$ while, the FID signal after steady-state saturation is exponential.

ACKNOWLEDGMENT

This work has been made possible by financial support from INTAS, Grant No. 93-2492, and was carried out within the research program of International Center for Fundamental Physics in Moscow.

[1] R. Boscaino, F.M. Gelardi, and R.N. Mantegna, Phys. Lett. A **124**, 373 (1987).
[2] R.G. DeVoe and R.G. Brewer, Phys. Rev. Lett. **50**, 1269 (1983).
[3] A. Szabo and T. Muramoto, Phys. Rev. A **39**, 3992 (1989).
[4] R. Boscaino and V.M. La Bella, Phys. Rev. A **41**, 5171 (1990).
[5] T. Muramoto and A. Szabo, Phys. Rev. A **38**, 5928 (1988).
[6] A. Szabo and R. Kaarli, Phys. Rev. B **44**, 12307 (1991).
[7] T. Endo, T. Muramoto, and T. Hashi, Opt. Commun. **51**, 163 (1984).

[8] E. Hanamura, J. Phys. Soc. Jpn. **52**, 3678 (1983).
[9] A. Schenzle, M. Mitsunaga, R.G. DeVoe, and R.G. Brewer, Phys. Rev. A **30**, 325 (1984).
[10] M. Yamanoi and J.H. Eberly, J. Opt. Soc. Am. B **1** 751 (1984).
[11] P.A. Apanasevich, S.Ya. Kilin, A.P. Nizovtsev, and N.S. Onischenko, Opt.Commun. **52**, 279 (1984).
[12] P.A. Apanasevich, S.Ya. Kilin, A.P. Nizovtsev, and N.S. Onischenko, J. Opt. Soc. Am. B **3** 587 (1986).
[13] S.Ya. Kilin and A.P. Nizovtsev, J. Phys. B **19**, 3457 (1986).
[14] A.I. Burshtein and V.S. Malinovsky, J. Opt. Soc. Am. B **8**, 1098 (1991).
[15] J. Javanainen, Opt. Commun. **50**, 26 (1984).
[16] P.R. Berman and R.G. Brewer, Phys. Rev. A **32**, 2784 (1985).
[17] A.R. Kessel, R.N. Shahmuratov, and L.D. Eskin, Zh. Éksp. Teor. Fiz. **94**, 202 (1988) [Sov. Phys. JETP **69**, 1164 (1989)].
[18] A.I. Burshtein, A.A. Zharikov, and V.S. Malinovsky, Phys. Rev. A **43**, 1538 (1991).
[19] K. Wodkiewicz and J.H. Eberly, Phys. Rev. A **32**, 992 (1985).
[20] V.S. Malinovsky, Opt. Spektrosk. **70**, 681 (1991) [Opt Spectrosc. (USSR) **70**, 399 (1991)].
[21] G.S. Agarwal, Z. Physik B **33**, 111 (1979).
[22] S.Ya. Kilin and A.P. Nizovtsev, Phys. Rev. A **42**, 4403 (1990).
[23] A.I. Burshtein, *Lectures on Quantum Kinetics* (NSU, Novosibirsk, 1968).
[24] G.M. Zhidomirov and K.M. Salihov, Zh. Éksp. Teor. Fiz. **56** 1933 (1969) [Sov. Phys. JETP. **29**, 1037 (1969)].
[25] P.R. Berman, J. Opt. Soc. Am. B **3**, 572 (1986).
[26] See, for example, L. Allen and J.H. Eberly, *Optical Resonance and Two-Level Atoms* (Wiley, New York, 1975).
[27] F.A. Hopf and M.O. Scally, Phys. Rev. **179**, 399 (1969).
[28] A. Schenzle, N.C. Wong, and R.G. Brewer, Phys. Rev. A **21**, 887 (1980).
[29] A. Schenzle, N.C. Wong, and R.G. Brewer, Phys. Rev. A **22**, 635 (1980).
[30] R.G. Brewer and R.L. Shoemaker, Phys. Rev. A **6**, 2001 (1972).
[31] H. Stehfest, Commun. ACM **13**, 47 (1970).